Composition of quartzite from the Ataneq fault, southern West Greenland

Possible source for ultrapure quartz?

Christian Knudsen

GEUS

Composition of quartzite from the Ataneq fault, southern West Greenland

Possible source for ultrapure quartz?

Christian Knudsen

Summary

Quartzite from the Ataneq fault have been analysed for the bulk chemical composition and for its mineral content.

The Ataneq fault zone is ca. 50 m thick, but the part which consists of pure quartzite is less. The samples analysed in the present report are collected in a zone that is approximately 50 m thick with the most pure quartzite in the centre of this zone. However, the degree of out-crop is not very good in the Ataneq fault zone which appears as a valley in the Greenlandic landscape.

The visited locality is located approximately 3 km from tidal water.

The main impurities are plagioclase, epidote, chlorite, muscovite, titanite, apatite and zir-con. Locally K-feldspar is common.

The grain-size is very variable. The quartz show clear signs of the deformation history and the quartz generally occur in a mylonite texture with a fine grain-size or as larger aggre-gates of quartz consisting of smaller sub-grains. The grain-size of the quartz varies with the amount of impurities in the rock – finer where there are many impurities. The plagioclase is relatively coarse compared to the other minerals often in the range 100 to 500 µ. The grain-size of the epidote is very variable from 1 to 50 µ. Muscovite and chlorite varies from ca. 200 µ long and 30 µ thick crystal down to 5 µ micron long and 1 µ thick crystals.

The fault-zone has probably been active over a long time span in the geological history mainly during early Proterozoic time (2.5 Ga (billion) to 1.6 Ga years ago). The quartz en-richment is interpreted as formed by hydrothermal processes in the fault-zone and de-formed under greenschist facies metamorphic conditions subsequently.

Content

Introduction

This report is made by GEUS as part of cooperation with North Cape Minerals (NCM).

Objective

The aim of the work is to describe the composition of a quartzite body that occur at the Ataneq fault ca. 5 km east of Innajatoq in the northern part of Godthåbsfjorden (Figure 1).

Background

The context is that NCM want to identify a quartz resource in Greenland which can be used for "high tech" purposes such as solar panels. The specifications are ca. < 1 ppm B, < 1 ppm P, < 1 ppm Fe, < 5 ppm Na+K, < 10 ppm Ti, < 25 ppm Al.

4 samples collected by GEUS in West Greenland was analysed at NGU using Laser Ablation ICP-MS was completed in 2009 (Table 1).

Table 1 Composition of 4 quartz-samples from Greenland. Values in ppm. NGU analysis.

Locality	GGU nr	B	P	Ti	Al	Li	Fe	Mn	Na	K	Ca	Ge	Rb	Sr	Be
Nalunaq	473741	1,5	3,9	10,9	18,9	5,5	1,7	0,4	<11,2	<2,3	<36,0	0,8	<0,04	<0,01	<0,13
Nalunaq	473741	4,3	5,2	6,3	11,5	6,5	<1,2	0,2	<11,2	<2,3	<36,0	0,8	<0,04	0,02	0,3
Ivigtut	343001	2,9	2,6	4,8	84,3	5,7	<1,2	0,5	116,9	35,2	<36,0	2,7	1,57	0,20	0,4
Ivigtut	343001	1,3	3,8	3,5	53,1	4,9	<1,2	<0,1	44,6	21,7	<36,0	2,4	0,61	0,04	0,7
Igaliko	473742	0,5	1,9	<1,8	<6,6	1,5	<1,2	0,2	<11,2	<2,3	<36,0	<0,1	0,05	<0,01	<0,13
Igaliko	473742	0,2	3,6	<1,8	38,3	11,7	<1,2	<0,1	75,6	8,7	<36,0	<0,1	0,15	0,06	0,3
Ataneq	499094	0,3	4,7	<1,8	<6,6	1,4	<1,2	0,5	<11,2	3,9	<36,0	0,3	0,08	0,18	0,3
Ataneq	499094	0,5	4,7	<1,8	<6,6	<0,2	<1,2	0,1	<11,2	3,0	<36,0	<0,1	<0,04	0,18	0,7
Detection limit		**0,21**	**1,75**	**1,84**	**6,63**	**0,16**	**1,19**	**0,09**	**11,17**	**2,34**	**35,97**	**0,12**	**0,04**	**0,01**	**0,13**

Based on the results of this small investigation, it was decided to focus on the quartzite in the Ataneq fault.

During the summer 2009 Christian Knudsen (GEUS) visited the quartzite at Ataneq together with Henrik Stendal (Råstof Direktoratet, Nuuk). During this visit 8 new samples were collected for further studies (GEUS no 473780 to 473787).

Geological setting

The quartz mylonite was mapped by J.F.W. Park in the 1980'ties (Park, 1986) and is represented on the 1:100.000 geological map Ivisartoq from the area (Chadwick & Coe, 1988). The fault is referred to as the Ataneq fault, and it was noted that the fault-zone is sicified.

The fault is assumed to be of early Proterozoic age with a ca. 4 km sub horizontal dextral (right-lateral) slip, and localising the "precipitation of considerable volumes of quartz from fluids moving through the fault zone". The present day appearance was formed by subsequent ductile deformation of the quartz-rich rocks in the fault zone.

At the locality visited in 2009, the Ataneq fault cut across gneisses of Archaean age and tonalitic composition belonging to the Taserssuaq tonalite complex (pink on Figure 1) which is part of the ca. 3 Ga. old Akia terraine (Garde, 1997). The tonalitic gneiss is a grey rock consisting of quartz, plagioclase and biotite with minor amounts of K-feldspar, hornblende, magnetite, ilmenite, apatite and zircon. The gneiss locally contains amphibolite and ultramafic lenses and pods.

Further to the north-east of the investigated locality (red star on Figure 1), the fault divides Akia terrain gneisses to the west from tonalitic gneisses belonging to a number of different terranes of 3.8 – 3.6 Ga (Isukassia & Færingehavn terrain), ca. 3 Ga (Kapisillit terraine) and 2.8 Ga (Tre Brødre terrain) to the east (Friend & Nutman 2005). However, there is also gneisses belonging to the Taserssuaq tonalite complex east of the fault, so it is not a terraine boundary as such (van Gool in Hollis et al., 2006).

Figure 1   Geological map of the Nuuk area. Red star is the quartzite locality described here. The map is ca. 100 km east to west.

Smith & Dymek (1983) think that the Ataneq is of similar age as the Proterozoic Kobbefjord Fault Zone (KFZ) which is described as a dextral NE-SW trending fault. The KFZ contain quartz-rich mylonites also containing feldspar, biotite, chlorite, epidote and muscovite and metamorphosed under greenschist facies conditions.

The Ataneq Fault was investigated by GEUS in 2005 during regional mapping and an evaluation of the gold potential tied to hydrothermal alteration in the fault-zone (Hollis et al. 2006). During this fieldwork the sample 499094 was collected.

During this 2005 fieldwork, it was found that the hydrothermal system tied to the Ataneq Fault is generally barren with no metal mineralisations. It was further found, that the fault itself is characterised by a low magnetic properties (Gulbrandsen in Hollis et al. 2006). The Ataneq Fault is described as a complex fault system consisting of more conjugating fault systems, of which the largest is ca. 50 to 75 m wide (Thøgersen in Hollis et al. 2006).

The Ataneq fault can be followed ca. 100 kilometres. It is trending north-east southwest, and is a pronounced feature (valley) in the landscape (Figure 2 and 3):

Figure 2 The Ataneq fault zone seen from a helicopter towards NE.

The Ataneq fault zone is ca. 50 m thick, but the part which consists of pure quartzite is less. The samples analysed in the present report are collected in a zone that is approximately 50 m thick with the most pure quartzite in the centre of this zone. However, the degree of out-crop is not very good (Figure 2 and 3) in the Ataneq fault zone which appear as a valley.

Figure 3 Ataneq fault zone. Henrik Stendal is standing on the quartzite.

Figure 4 Pure quartzite from the central part of the fault zone.

Figure 5 Pure quartzite with the typical light greenish tint.

Figure 6 Red stained, feldspar rich quartzite from the marginal part of the fault-zone.

Figure 7 Light coloured quartzite from the marginal part of the fault-zone.

As can be seen on Figures 4, 5, 6 & 7, the rock is very fine-grained, and the individual mineral grains can not be identified with the unaided eye.
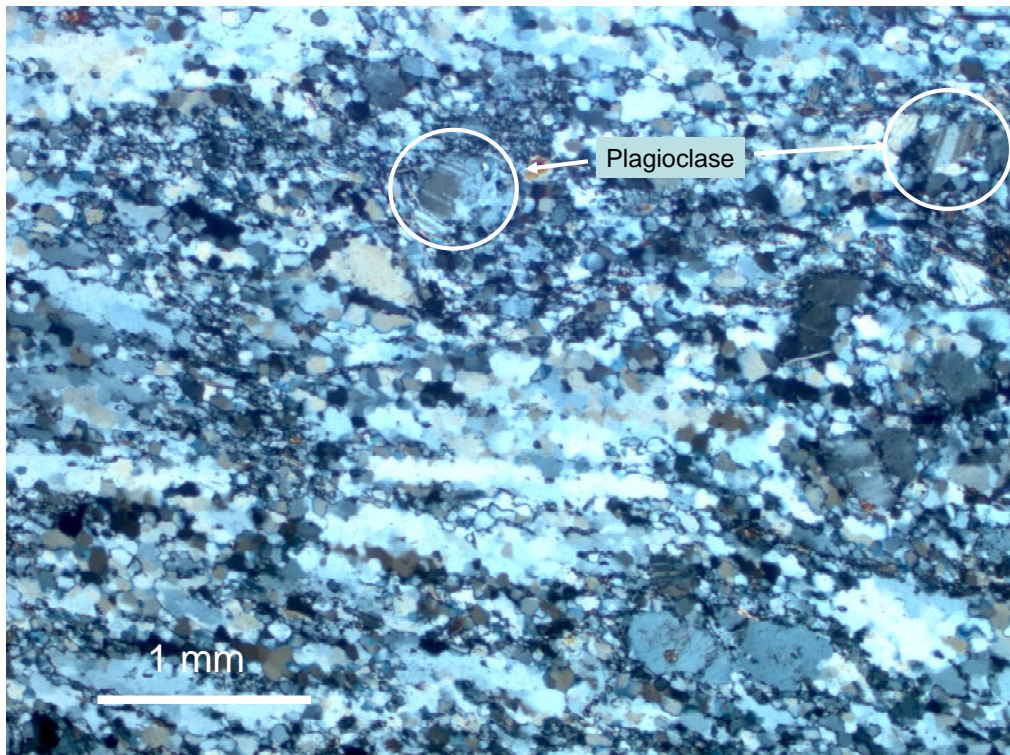

Figure 8   Sample 499094. Photomicrograph (optical microscope), crossed nicholls (polarising filters).

Under the microscope the mylonitic texture of the rock can be observed (Figure 8). The quartz is fine-grained or occurs as elongated aggregates consisting of sub-grains with a typical grain-size of 30 to 50 µ (Figure 9). However, the grain-size varies somewhat depending on the variable content of impurities – with finer grain-size where the content of impurities is high (Figure 8). Plagioclase is common and is easily recognised on the microphotograph by the albite twinning (Figure 8, parallel light and dark lamellae). The plagioclase crystals are typically 100 to 500 µ.
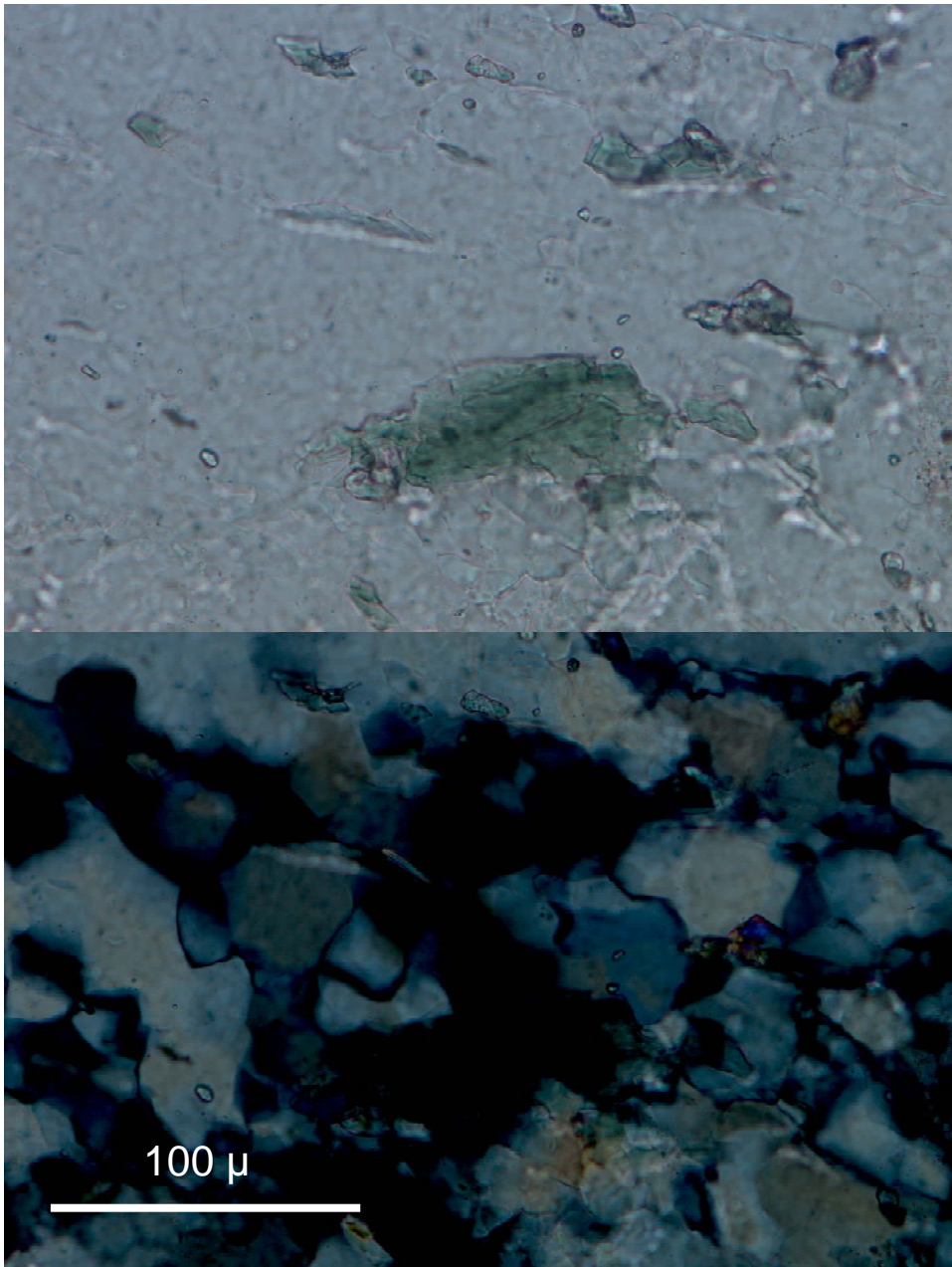


Figure 9   Sample 499094. Photomicrograph, the lower half represents the same area as upper but with crossed nicholls.

On Figure 9, the green colour of the epidote is seen together with the variable grain-size of the epidote.

Methods

The samples have been analysed for their bulk rock composition at ACME laboratories in Canada and the mineral chemistry have been analysed using an Electron Microprobe at Institute for Geography and Geology at University of Copenhagen.

Chemical bulk rock analysis

Sample Preparation
Rock samples are jaw crushed to 80% passing 10 mesh (2 mm), a 250 g aliquot is riffle split and pulverized to 85% passing 200 mesh (75 ⌈m) in a mild-steel ring-and-puck mill.

Sample Digestion
A 0.2 g aliquot is weighed into a graphite crucible and mixed with 1.5 g of $LiBO_2/Li_2B_4O_7$ flux. Crucibles are placed in an oven and heated to 980°C for 30 minutes. The cooled bead is dissolved in 5% HNO_3 (ACS grade nitric acid diluted in demineralised water). Calibration standards and reagent blanks are added to the sample sequence.

Sample Analysis
Sample solutions are aspirated into an ICP emission spectrograph (Spectro Ciros Vision or Varian 735) for the determination of the following 11 major and minor oxides and 32 elements: SiO_2, Al_2O_3, Fe_2O_3, CaO, MgO, Na_2O, K_2O, MnO, TiO_2, P_2O_5, and Cr2O3. Sc, V, Cr, Co, Ni, Cu, Zn, Rb, Sr, Y, Zr, Nb, Cs, Ba, La, Ce, Pr, Nd, Sm, Eu, Gd, Tb, Dy, Ho, Er, Tm, Yb, Lu, Hf, Pb, Th and U. Loss on ignition (LOI) is determined for both packages by igniting a 1 g sample split at 950°C for 90 minutes then measuring the weight loss. Total Carbon and Sulphur are determined by the Leco method. Total carbon and sulphur analysis by Leco oven.

Microprobe analysis

The microprobe analysis was performed using a JEOL JXA-8200 Superprobe. The instrument has 5 wavelength dispersive spectrometers. The acceleration voltage was set to 25 kV and the beam current to 25 nA.

Results

Chemical results

The major and minor elements results are tabulated in Table 2 (full analysis is given in Appendix 1).

Table 2   Major and minor elements

	473780	473781	473782	473783	473784	473785	473786	473787	499094
SiO2	97,24	96,74	92,3	97,58	96,53	98,04	95,04	97,93	96,37
Al2O3	0,86	1,16	3,47	0,47	0,6	0,48	2,28	0,72	1,64
Fe2O3	0,44	0,57	0,59	0,47	1,12	0,34	0,4	0,35	0,34
MgO	0,04	0,08	0,04	0,06	0,07	0,06	0,04	0,04	0,07
CaO	0,29	0,27	0,58	0,27	0,33	0,18	0,25	0,14	0,13
Na2O	0,2	0,45	0,98	0,02	0,11	0,1	1,1	0,3	0,75
K2O	0,08	0,06	0,99	0,06	0,01	0,06	0,08	<0.01	0,09
TiO2	0,01	0,03	0,02	0,02	0,02	0,02	0,02	0,01	0,02
P2O5	0,01	0,02	0,02	0,02	0,02	0,02	0,03	<0.01	0,02
MnO	<0.01	<0.01	<0.01	<0.01	0,01	<0.01	<0.01	<0.01	<0.01
LOI	0,8	0,6	0,9	1	1,2	0,7	0,8	0,5	0,6
Sum	99,97	99,98	99,89	99,97	100,02	100,00	100,04	99,99	100,03

Most of the impurities in the quartzite are Al bearing silicates such as plagioclase, chlorite, muscovite and epidote. However, as the correlation or trend-line (Figure 10) cut the x-axis at ca. 99 % suggesting the presence of other impurities than alumino-silicates in the quartzite.


$$y = -0.54 x + 53.2$$
$$R^2 = 0.92$$
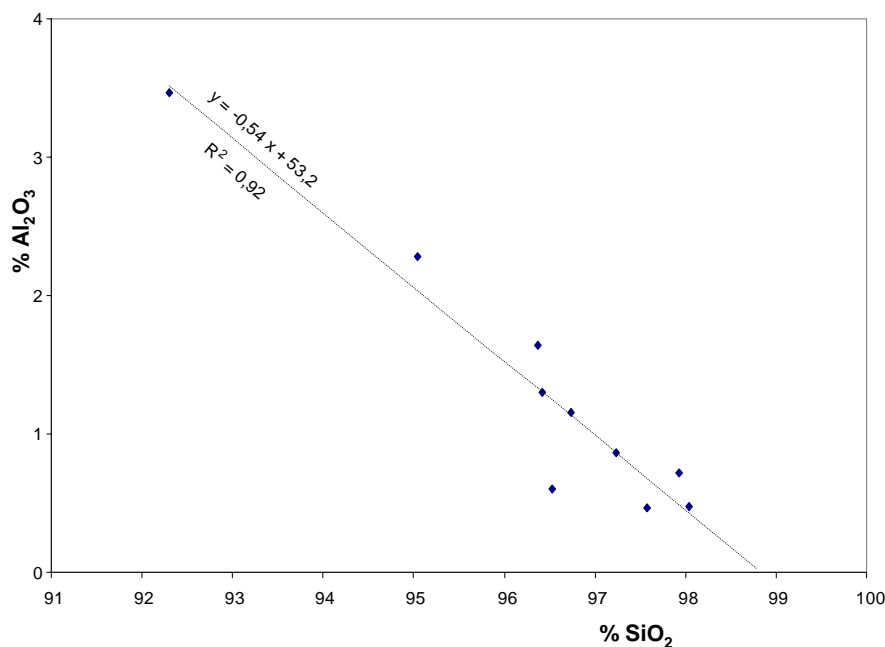
Figure 10 Al_2O_3 versus SiO_2
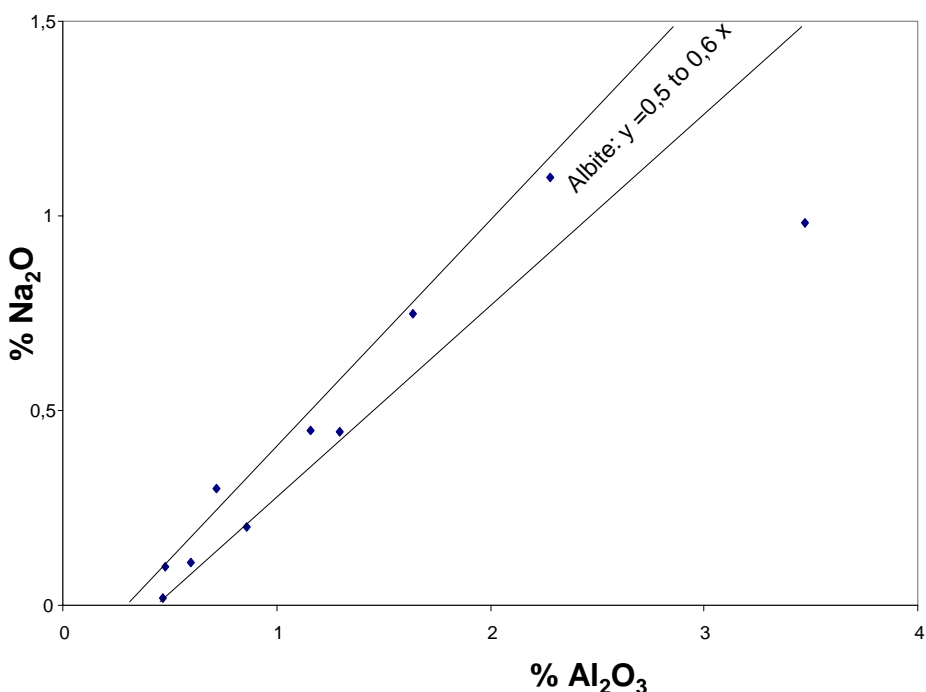
Figure 11 Na$_2$O versus Al$_2$O$_3$

On Figure 11 it can be seen, that the main variation in the aluminium content can be explained by varying content of albite. One sample has high aluminium content (473782) combined with a high content of e.g. potassium now in K-feldspar and muscovite/sericite.

The chemical analysis can be used to calculate the theoretical mineralogical composition of a rock if you assume that it was crystallized from a melt (the "CIPW norm", Table 3). This will not give a correct composition of metamorphic rocks such as these, as the igneous minerals have recrystallised to other typical for the "greenschist facies" but the CIPW will however give a good hint of the overall content of non quartz components in the rock.

Table 3 CIPW norm

	473780	473781	473782	473783	473784	473785	473786	473787	499094
Quartz	95,7	93,6	82,2	97,4	95,7	97,3	88,3	96,1	91,7
Plagioclase	2,9	4,8	10,6	1,2	2,1	1,5	10,4	3,1	6,9
Orthoclase	0,5	0,4	5,9	0,4	0,1	0,4	0,5	0,1	0,5
Corundum	0	0	0	0	0	0	0	0	0,13
Diopside	0,1	0,2	0,5	0,1	0,3	0,1	0	0,04	0
Hypersthene	0,7	0,9	0,6	0,7	1,6	0,6	0,7	0,6	0,7
Ilmenite	0,02	0,06	0,04	0,04	0,04	0,04	0,04	0,02	0,04
Magnetite	0,06	0,09	0,09	0,07	0,16	0,04	0,06	0,06	0,04
Apatite	0,02	0,05	0,05	0,05	0,05	0,05	0,07	0,02	0,05

Minerals such as diopside, hyperstene, ilmenite and magnetite are not likely to be preserved in metamorphic rocks like these quartzite's, and the magnesium, iron, titanium, calcium etc. are likely to be distributed into minerals such as chlorite, epidote and titanite.

Microprobe results

5 polished thin sections have been investigated using the microprobe. The microprobe electron backscatter images are enclosed in Appendix 2 and the analytical results are included in Appendix 3.

Apart from quartz, albite is the most common mineral. An estimate of the content can be taken from Table 2 as albite (plagioclase) is the main Na bearing mineral found in the rock.

There are two green minerals in the rock both contributing to the common light green colour of the rock (Figure 5), namely epidote and chlorite.
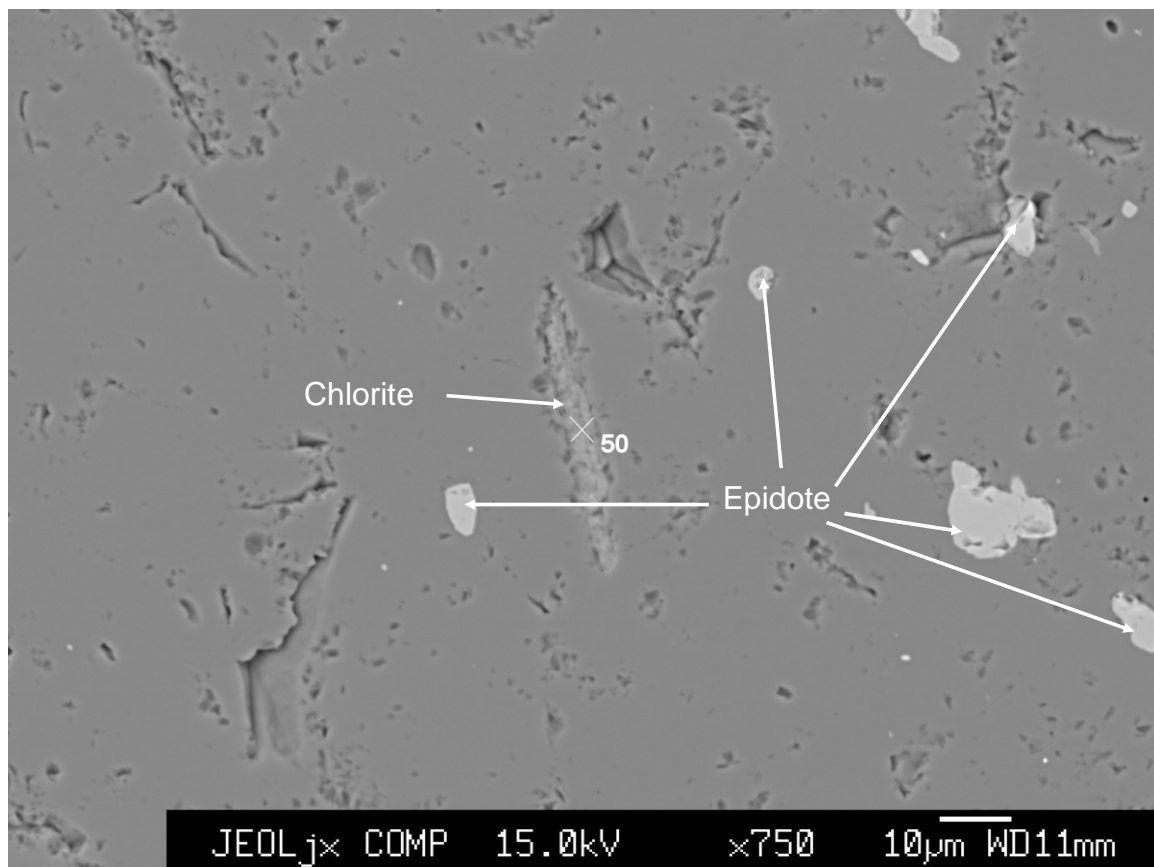
Figure 12   Electron backscatter image of sample 473784. Length of scale bar is 10 μ. An electron backscatter image shows the average atomic weight of the elements consisting the minerals and the more heavy the lighter the grains on the image. The main (grey) mineral is quartz.

On Figure 12, the grain-size of the epidote is between ca. 1 to 10 μ and the chlorite crystal is ca. 30 μ long and ca. 5 μ wide. The grain-size of the epidote may be up to 50 μ and the chlorite crystals may also be even coarser (ca. 100 μ). Chlorite is a sheet silicate and occurs as flaky grains as seen on Figure 12.

As can be seen on Figure 12, there are some very small grains (< 1 µ light spots). These probably represent epidote judged from their grey tone, but as they are considerably smaller that the electron beam diameter, they can not be analysed using the microprobe.
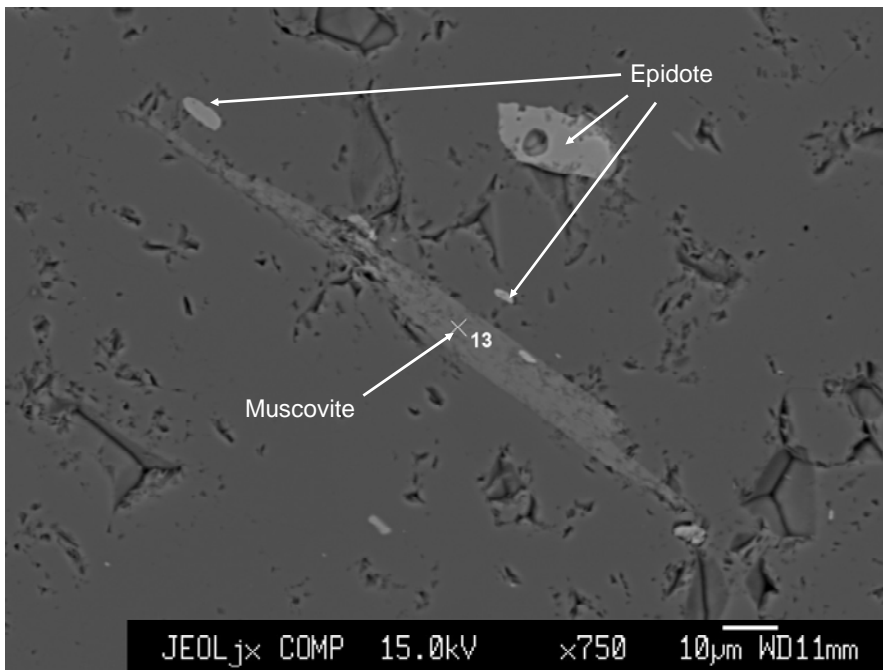
Figure 13 Sample 473785. Muscovite and epidote in quartz.
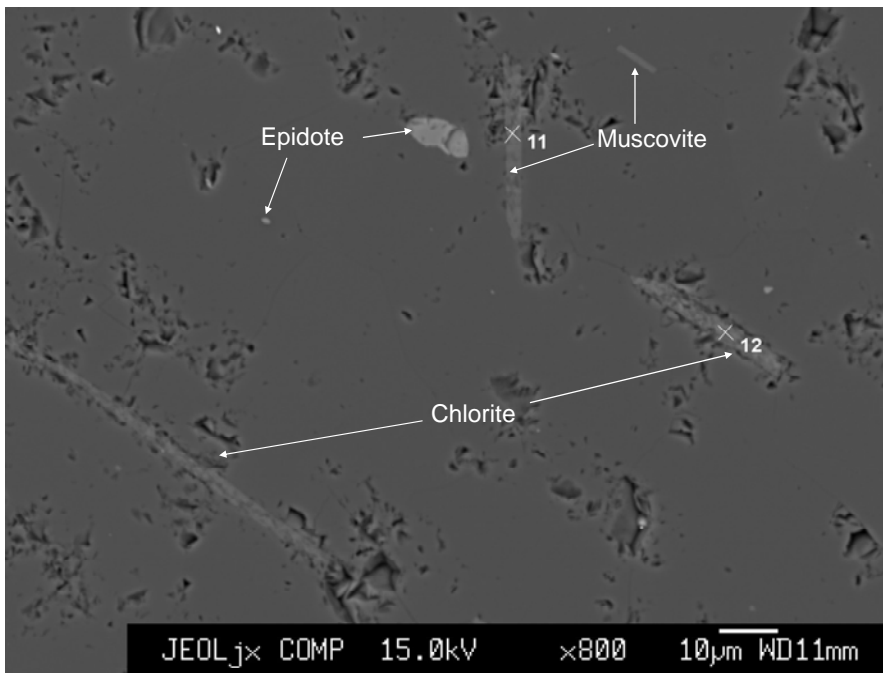
Figure 14   Sample 473785. Muscovite, chlorite and epidote in quartz.

Muscovite is also a common mineral in the rock (Figure 13 and 14). It is also a sheet silicate occurring as flaky grains with a grain-size from ca. 10 µ long and 1 µ wide (thick) to 100 µ and 10 µ wide.
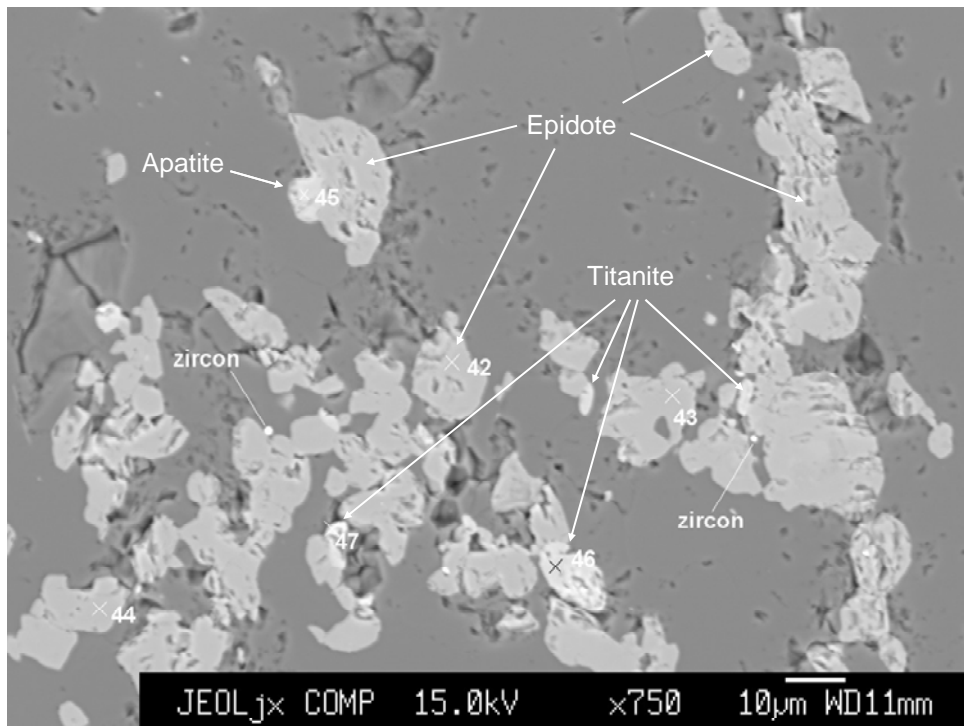
Figure 15 Sample 473784. An epidote-rich aggregate I quartz. There are minor amounts of titanite (sphene) as well as apatite and zircon.

References

Chadwick, B & Coe, K, 1988: Ivisârtoq 64 V.2 Nord. 1:100.000 geological map. GGU.

Friend, C.R.L. & Nutman, A.P. 2005: New pieces to the Archaean terrain jigsaw puzzle in the Nuuk region, southern West Greenland: steps in transforming a simple insight into a complex regional tectonothermal model. Jour. Geol. Soc. 162. 147-162.

Garde, A. A. 1997: Accretion and evolution of an Archaean high-grade grey gneiss – amphibolite complex: the Fiskefjord area, southern West Greenland. Geology of Greenland Survey Bulletin 177.

Hollis, J., Schmid, S., Stendal, H., van Gool, J.A.M. & Weng, W. 2006: Supracrustal belts in Godthåbsfjord region, southern West Greenland. GEUS Rapport 2006/7.

Park, J.F.W. 1986: Fault systems in the inner Godthåbsfjord region of the Archaean block, southern West Greenland. Unpubl. Thesis. University of Exeter.

Smith G.M. and Dymek R.F. 1983: A description and interpretation of the Proterozoic Kobbefjord Fault Zone, Godthab district, West Greenland. *Rapport - Grønlands Geologiske Undersøgelse* **112** (1983), pp. 113–127.

Appendix 1

		Unit	Limit of detection	473780	473781	473782	473783	473784	473785	473786	473787	499094
SiO2	%	0,01	97,24	96,74	92,3	97,58	96,53	98,04	95,04	97,93	96,37
Al2O3	%	0,01	0,86	1,16	3,47	0,47	0,6	0,48	2,28	0,72	1,64
Fe2O3	%	0,04	0,44	0,57	0,59	0,47	1,12	0,34	0,4	0,35	0,34
MgO	%	0,01	0,04	0,08	0,04	0,06	0,07	0,06	0,04	0,04	0,07
CaO	%	0,01	0,29	0,27	0,58	0,27	0,33	0,18	0,25	0,14	0,13
Na2O	%	0,01	0,2	0,45	0,98	0,02	0,11	0,1	1,1	0,3	0,75
K2O	%	0,01	0,08	0,06	0,99	0,06	0,01	0,06	0,08	<0.01	0,09
TiO2	%	0,01	0,01	0,03	0,02	0,02	0,02	0,02	0,02	0,01	0,02
P2O5	%	0,01	0,01	0,02	0,02	0,02	0,02	0,02	0,03	<0.01	0,02
MnO	%	0,01	<0.01	<0.01	<0.01	<0.01	0,01	<0.01	<0.01	<0.01	<0.01
Cr2O3	%	0,002	0,01	0,012	0,008	0,007	0,008	0,008	0,005	0,007	0,007
LOI	%		0,8	0,6	0,9	1	1,2	0,7	0,8	0,5	0,6
Sum	%	0,01	99,98	99,99	99,93	99,99	99,99	100,02	100	100,02	100,01
TOT/C	%	0,02	<0.02	0,3	<0.02	<0.02	<0.02	<0.02	0,04	<0.02	<0.02
TOT/S	%	0,02	<0.02	<0.02	<0.02	<0.02	<0.02	<0.02	<0.02	<0.02	<0.02
Ba	ppm	1	48	4	393	15	6	13	12	7	39
Co	ppm	0,2	0,8	1,7	0,6	1,1	1,2	0,7	0,5	0,6	0,6
Ga	ppm	0,5	1,9	2,2	5	2,1	2,1	1,8	2	1,2	1,6
Hf	ppm	0,1	0,2	0,6	0,4	0,2	0,3	<0.1	0,5	0,3	0,4
Nb	ppm	0,1	0,1	0,1	0,1	<0.1	0,5	0,1	0,1	0,1	0,4
Rb	ppm	0,1	2,8	1,4	16,4	1,9	0,9	1,5	1,5	0,5	2,4
Sr	ppm	0,5	39,2	34,2	118,7	37,7	46,8	26,5	39,6	16,4	25,7
Th	ppm	0,2	<0.2	0,4	0,9	<0.2	0,2	0,4	0,3	<0.2	<0.2
U	ppm	0,1	<0.1	<0.1	0,1	<0.1	<0.1	<0.1	<0.1	<0.1	<0.1
V	ppm	8	64	52	54	41	34	27	25	22	14
Zr	ppm	0,1	4,5	10,9	13,4	3,6	11,3	9,2	9,9	4,9	12,1
Y	ppm	0,1	0,6	0,6	0,7	0,3	0,7	0,5	0,6	0,4	0,3
La	ppm	0,1	0,9	2,7	4,2	0,5	2,7	2,1	1,7	1,2	1,2
Ce	ppm	0,1	1,9	4,9	7,5	1,2	5,6	5	3	2,3	1,8
Pr	ppm	0,02	0,22	0,53	0,76	0,12	0,58	0,48	0,32	0,22	0,16
Nd	ppm	0,3	0,7	1,6	2,1	0,4	1,6	1,5	1,1	0,6	0,6
Sm	ppm	0,05	<0.05	0,13	0,14	0,07	0,21	0,08	0,05	0,06	<0.05
Eu	ppm	0,02	0,05	0,08	0,14	0,06	0,07	0,07	0,08	0,04	0,07
Gd	ppm	0,05	0,09	0,12	0,17	0,08	0,21	0,16	0,13	0,1	0,14
Tb	ppm	0,01	0,03	0,03	0,03	0,02	0,03	0,02	0,02	0,03	0,01
Dy	ppm	0,05	0,14	0,24	0,26	0,19	0,17	0,16	0,22	0,16	0,15
Er	ppm	0,03	0,08	0,1	0,06	0,04	0,08	0,06	0,06	0,1	0,07
Yb	ppm	0,05	<0.05	0,18	<0.05	0,08	<0.05	0,07	0,08	<0.05	<0.05
Mo	ppm	0,1	0,1	<0.1	<0.1	<0.1	0,2	<0.1	<0.1	0,1	0,1
Cu	ppm	0,1	1,6	0,7	2,1	47,7	2,5	1,4	1,2	1,6	0,9
Pb	ppm	0,1	0,6	0,3	0,8	0,4	0,4	0,2	0,3	0,2	0,2
Zn	ppm	1	1	2	2	2	2	2	1	2	1
Ni	ppm	0,1	0,9	1,3	0,8	1,4	2,8	1,4	0,9	1,2	1,5
Au	ppb	0,5	0,7	1,7	<0.5	1,9	<0.5	0,8	<0.5	0,5	<0.5

Appendix 2

473780 Quartzite
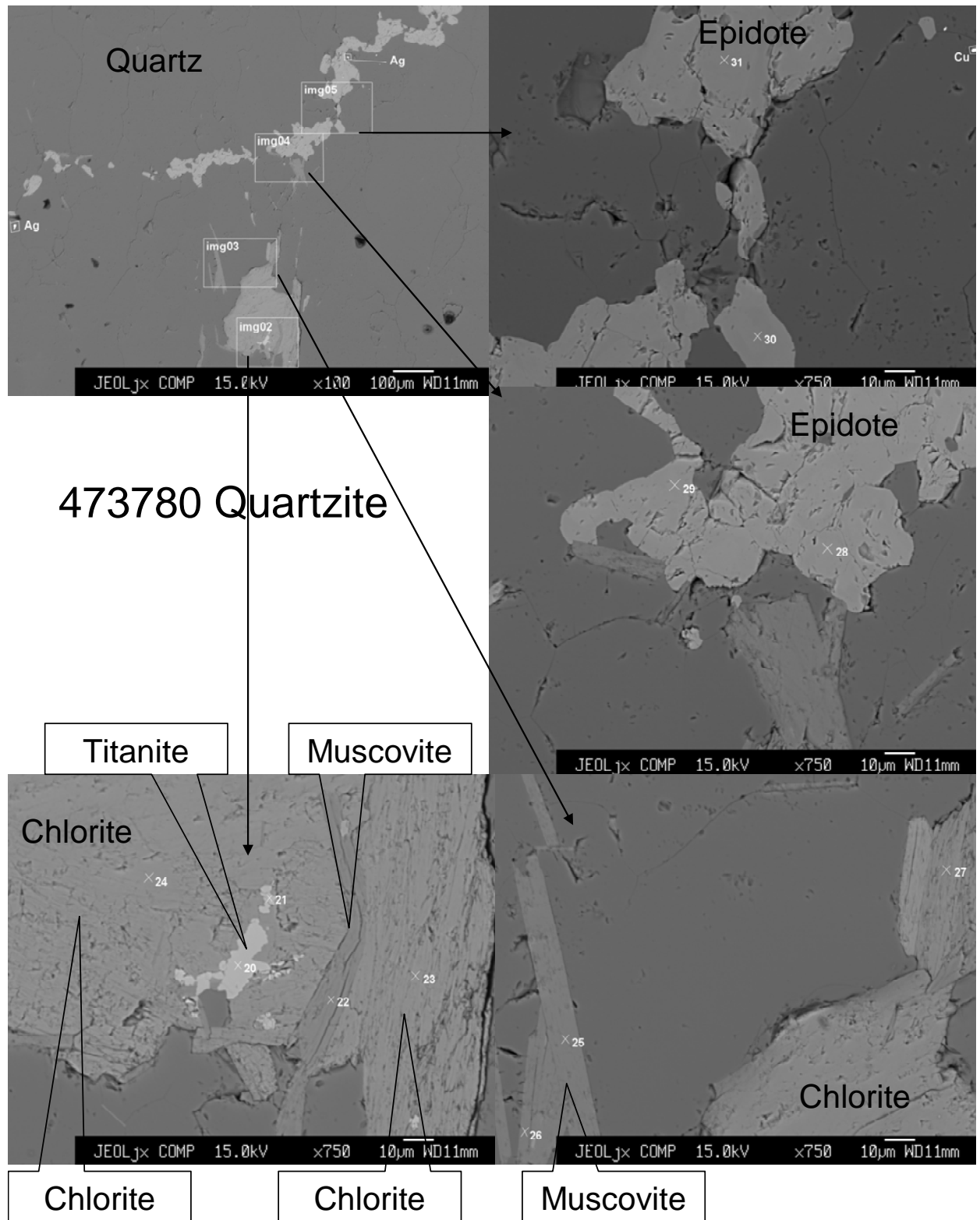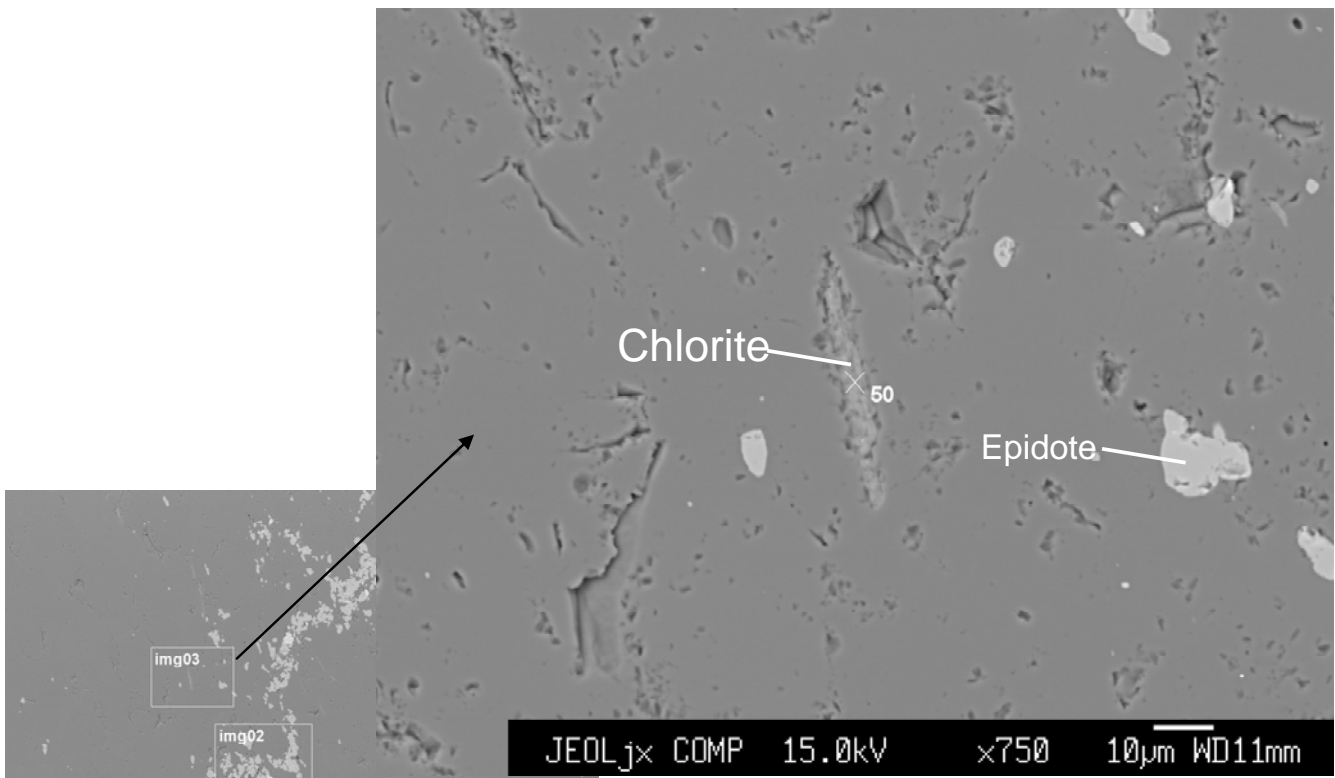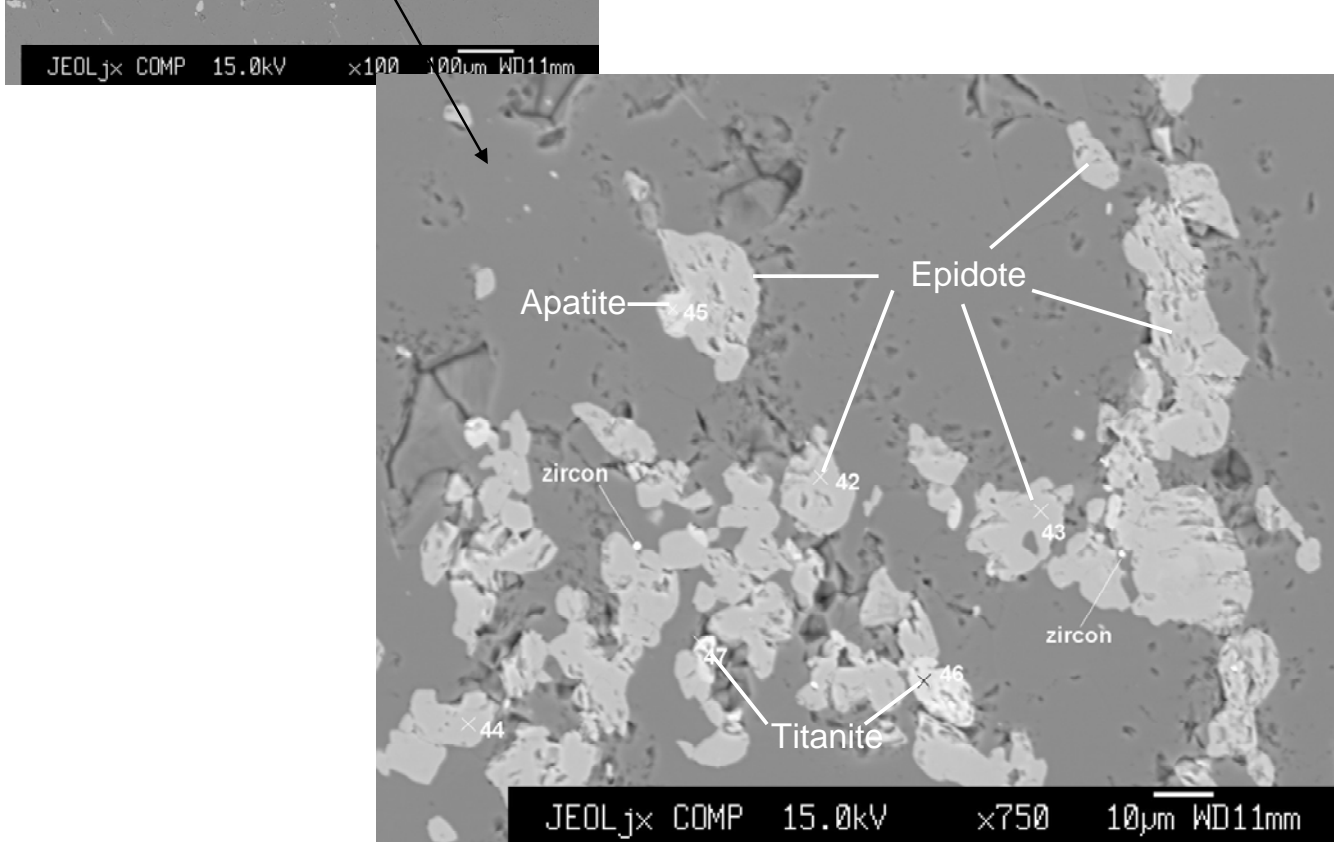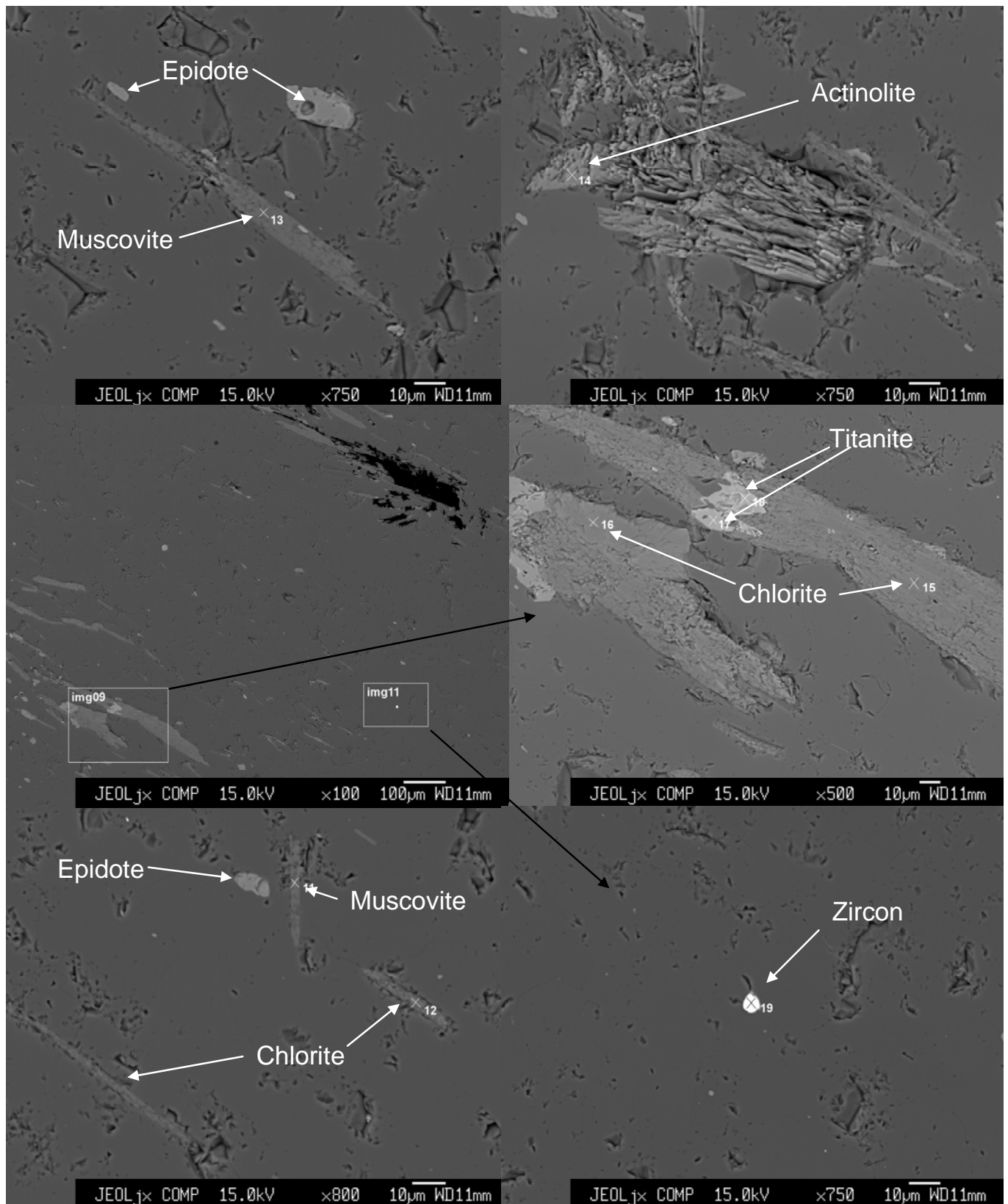
473784

473785

473787
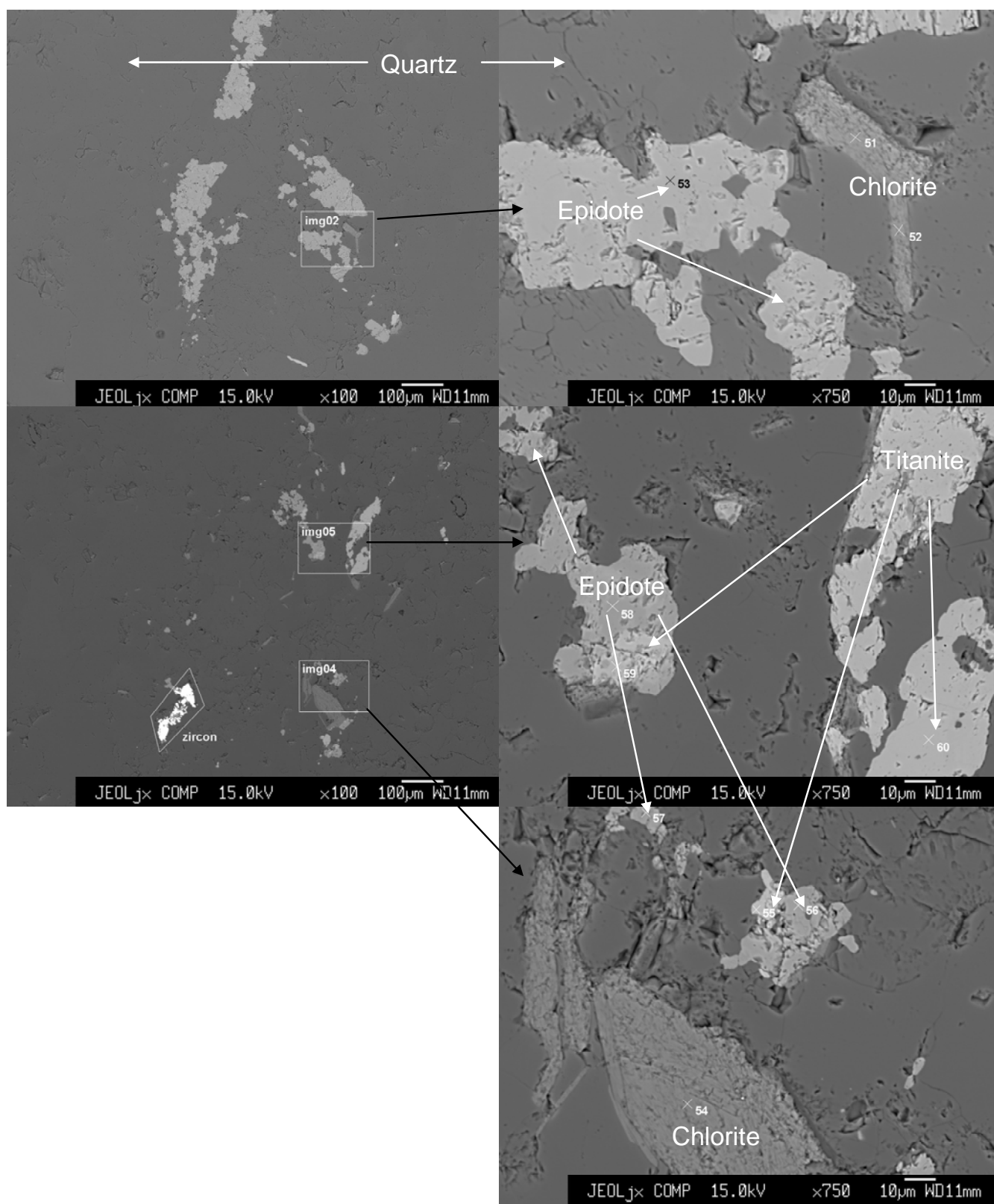
Appendix 3

Sample	SiO2	TiO2	Al2O3	FeO	MnO	MgO	CaO	Na2O	K2O	Total	Comment
473780	50,4	0,2	31,1	3,2	0,09	2,7	0,00	0,12	8,0	95,75	Muscovite
473780	49,0	0,3	32,1	2,6	0,01	2,3	0,00	0,33	10,1	96,76	Muscovite
473780	48,0	0,3	28,3	3,3	0,01	3,2	0,00	0,16	10,8	94,01	Muscovite
473785	49,6	0,2	29,6	3,1	0,01	2,9	0,45	0,30	10,1	96,19	Muscovite
473785	51,6	0,1	28,6	2,6	0,04	3,0	0,01	0,27	10,4	96,73	Muscovite
473785	49,8	0,4	30,9	2,8	0,07	2,8	0,03	0,22	10,7	97,61	Muscovite
499094	51,3	0,1	28,0	2,2	0,04	3,5	0,02	0,16	10,8	96,02	Muscovite
499094	49,9	0,1	28,4	2,9	0,00	3,2	0,00	0,13	10,4	95,12	Muscovite
Mean	49,9	0,2	29,6	2,8	0,0	2,9	0,1	0,2	10,2	96,0	Muscovite

Sample	SiO2	TiO2	Al2O3	FeO	MnO	MgO	CaO	Na2O	K2O	Total	Comment
473780	27,8	0,0	19,4	23,6	0,56	17,7	0,02	0,02	0,0	89,05	Chlorite
473780	28,0	0,1	21,6	23,2	0,44	16,8	0,01	0,02	0,0	90,06	Chlorite
473780	27,8	0,0	18,1	22,3	0,51	16,7	0,09	0,01	0,3	85,78	Chlorite
473784	28,3	0,0	21,4	16,8	0,44	22,2	0,04	0,00	0,0	89,20	Chlorite
473784	30,4	0,0	16,3	13,5	0,22	14,8	0,60	0,06	0,3	76,23	Chlorite
473784	28,0	0,1	20,4	16,4	0,38	21,8	0,06	0,02	0,0	87,18	Chlorite
473785	30,1	0,0	20,8	16,8	0,39	21,0	0,07	0,03	0,0	89,16	Chlorite
473785	29,5	0,0	19,9	18,5	0,40	21,1	0,11	0,03	0,0	89,57	Chlorite
473785	28,3	0,0	19,4	19,5	0,35	19,9	0,03	0,04	0,0	87,60	Chlorite
473787	24,4	0,0	17,0	18,4	0,30	21,8	0,08	0,02	0,0	82,08	Chlorite
473787	26,3	0,0	21,0	19,0	0,32	19,7	0,08	0,02	0,0	86,51	Chlorite
473787	26,8	0,0	19,7	19,4	0,32	20,8	0,06	0,00	0,0	87,11	Chlorite
Mean	28,0	0,0	19,6	19,0	0,4	19,5	0,1	0,0	0,1	86,6	Chlorite

Sample	SiO2	TiO2	Al2O3	FeO	MnO	MgO	CaO	Na2O	K2O	Total	Comment
473780	31,6	38,5	1,6	0,9	0,01	0,0	28,9	0,01	0,03	101,53	Titanite
473780	31,3	38,0	2,0	1,3	0,03	0,2	28,1	0,02	0,01	101,02	Titanite
473784	31,4	36,0	2,4	1,0	0,11	0,0	27,7	0,08	0,03	98,79	Titanite
473785	31,3	37,8	1,6	0,2	0,07	0,0	28,0	0,05	0,00	98,90	Titanite
473785	31,0	38,5	1,3	0,5	0,00	0,0	28,3	0,00	0,00	99,73	Titanite
473785	30,5	38,2	1,4	0,5	0,10	0,0	28,0	0,00	0,01	98,74	Titanite
473787	30,5	36,8	2,1	1,1	0,06	0,0	28,1	0,06	0,01	98,70	Titanite
473787	30,7	37,0	2,3	0,8	0,06	0,0	28,5	0,00	0,00	99,48	Titanite
473787	31,4	36,2	2,8	0,9	0,08	0,0	28,9	0,04	0,01	100,17	Titanite
499094	33,1	37,8	2,0	0,6	0,04	0,0	27,7	0,06	0,40	101,76	Titanite
499094	31,1	35,7	3,1	0,7	0,02	0,0	28,6	0,02	0,01	99,20	Titanite
499094	32,2	37,0	2,2	0,5	0,00	0,0	29,1	0,06	0,02	101,08	Titanite
Mean	31,3	37,3	2,1	0,7	0,0	0,0	28,3	0,0	0,0	99,9	Titanite

Sample	SiO2	TiO2	Al2O3	FeO	MnO	MgO	CaO	Na2O	K2O	Total	Comment
473780	38,7	0,1	25,6	10,0	0,15	0,0	23,4	0,02	0,0	97,95	Epidote
473780	38,2	0,1	25,0	9,8	0,21	0,0	23,5	0,03	0,0	96,79	Epidote
473780	38,8	0,1	25,6	9,4	0,06	0,0	23,7	0,00	0,0	97,56	Epidote
473780	38,6	0,1	25,7	9,7	0,19	0,0	23,8	0,00	0,0	98,08	Epidote
473784	38,6	0,1	24,8	10,0	0,11	0,0	23,1	0,04	0,0	96,71	Epidote
473784	38,3	0,1	24,9	9,7	0,21	0,0	23,5	0,00	0,0	96,66	Epidote
473784	37,0	0,1	24,3	10,1	0,17	0,0	23,4	0,02	0,0	95,03	Epidote
473785	38,4	0,1	25,0	9,1	0,22	0,0	23,0	0,00	0,0	95,87	Epidote
473785	36,8	0,0	23,5	10,2	0,15	0,0	22,9	0,02	0,0	93,63	Epidote
473785	37,9	0,1	24,7	9,7	0,12	0,0	22,9	0,01	0,0	95,45	Epidote
473785	38,7	0,0	25,0	9,5	0,11	0,0	23,0	0,00	0,0	96,41	Epidote
473785	38,2	0,0	25,1	10,1	0,07	0,0	23,1	0,00	0,0	96,60	Epidote
473785	38,5	0,0	25,3	9,3	0,16	0,0	23,1	0,02	0,0	96,45	Epidote
473787	38,4	0,0	23,5	11,4	0,12	0,0	23,6	0,04	0,0	97,05	Epidote
473787	38,8	0,1	22,9	12,5	0,35	0,0	22,9	0,02	0,0	97,52	Epidote
473787	38,8	0,1	23,7	11,4	0,11	0,3	22,6	0,01	0,0	97,10	Epidote
473787	38,2	0,5	22,8	12,3	0,10	0,1	23,3	0,03	0,0	97,33	Epidote
499094	38,9	0,0	24,9	10,1	0,19	0,0	23,2	0,00	0,3	97,61	Epidote
499094	38,1	0,1	24,0	11,8	0,15	0,0	23,3	0,00	0,1	97,55	Epidote
499094	38,2	0,1	24,2	10,2	0,03	0,0	23,6	0,03	0,1	96,41	Epidote
Mean	38,3	0,1	24,5	10,3	0,1	0,0	23,3	0,0	0,0	96,7	Epidote

Sample	SiO2	TiO2	Al2O3	FeO	MnO	MgO	CaO	Na2O	K2O	Total	Comment
473784	0,7	0,0	0,0	0,2	0,00	0,0	55,0	0,00	0,0	55,90	Apatite
499094	0,3	0,0	0,0	0,1	0,16	0,0	56,4	0,00	0,0	56,97	Apatite
499094	69,5	0,0	19,8	0,0	0,01	0,0	0,4	10,13	0,1	99,98	Albite
473785	36,9	0,0	0,0	0,0	0,00	0,0	0,0	0,00	0,0	36,99	Zircon
473785	53,9	0,0	0,4	9,7	0,38	17,2	12,9	0,08	0,0	94,65	Actinolite
473785	30,2	0,5	11,4	16,4	0,12	15,8	0,3	0,19	8,5	83,47	Biotite